

Rec'd APR 8 1946

494

T. N. 1009

FILE COPY

No. 1

NATIONAL ADVISORY COMMITTEE FOR AERONAUTICS

TECHNICAL NOTE

No. 1009

ANALYSIS OF DEEP RECTANGULAR SHEAR WEB ABOVE BUCKLING LOAD

By Samuel Levy, Ruth M. Woolley, and Josephine N. Corrick
National Bureau of Standards



Washington
March 1946

FILE COPY

To be Returned to the Files of
Ames Aeronautical Laboratory
National Advisory Committee
for Aeronautics
Moffett Field, Calif.

NATIONAL ADVISORY COMMITTEE FOR AERONAUTICS

TECHNICAL NOTE NO. 1009

ANALYSIS OF DEEP RECTANGULAR SHEAR WEB ABOVE BUCKLING LOAD

By Samuel Levy, Ruth M. Woolley, and Josephine N. Corrick

SUMMARY

A solution of Von Kármán's equations for plates with large deflections is presented for the case of a rectangular shear web with height-to-width ratio 2.5 reinforced by vertical struts having one-fourth the weight of the shear web. The results are compared with the solution of NACA TN No. 962 for a square shear web and with approximate analyses by Kuhn and by Langhaar.

The computed shear deformation differed not more than 2 percent from that for the square web. The stresses at the center and at the corners in line with the diagonal tension wrinkles and the force at the middle of the struts differed by not more than 30 percent from that for the square web. Kuhn's analysis gave values of shear deformation and of stresses that were up to 37 percent larger than those for the present analysis, and values for the maximum force in the struts that were smaller. Langhaar's analysis gave values for the shear deformations, stresses, and strut force that were generally much larger than those given by the present analysis; the differences were of the order of 50 to 400 percent at the largest load.

INTRODUCTION

An analysis of a square shear web above the buckling load was presented in reference 1. Actual shear webs are frequently rectangular rather than square, with a depth-width ratio considerably greater than 1. The analysis of reference 1 therefore was repeated for a shear web with depth/width = 2.5. Comparison of the results with those for the square web then would indicate the effect of changes in the depth-width ratio.

This investigation, conducted at the National Bureau of Standards, was sponsored by and conducted with the financial assistance of the National Advisory Committee for Aeronautics.

SYMBOLS

The symbols have the following significance (see fig. 1b):

x, y coordinate axes with origin at corner of plate

a length of plate in x -direction

$b = 2.5a$ length of plate in y -direction

h thickness of plate

w deflection of plate

E Young's modulus

$\mu = \sqrt{0.1} = 0.316$ Poisson's ratio

$D = Eh^3/12(1 - \mu^2)$ flexural rigidity of plate

F stress function

Q shear load carried by beam

$\bar{\sigma}_x$ average normal stress in plate in x -direction

$\bar{\sigma}_y$ average normal stress in plate in y -direction

τ median fiber shear stress at corners of plate

$r = 1/4$ ratio of strut weight to plate weight

P compressive force in strut

ϵ_x' , ϵ_y' , γ_{xy}' median fiber strains

σ_x' , σ_y' , τ_{xy}' median fiber stresses

σ_x'' , σ_y'' , τ_{xy}'' extreme fiber bending stresses

$\sigma_x, \sigma_y, \tau_{xy}$ extreme fiber stresses

$A_m, B_n, b_{m,n}$ coefficients in stress function

$w_{m,n}$ coefficient in deflection function

m, n integral numbers used as subscripts

$\bar{\gamma} = 2.632 \tau/E$ apparent shearing deformation of beam

u, v displacements in x - and y -directions, respectively

p lateral pressure in Von Kármán's equations

α angle between direction of maximum principal stress and x -axis

FUNDAMENTAL EQUATIONS

Consider an initially flat rectangular plate of uniform thickness. The two short edges are assumed to be simply supported by heavy flanges, integral with the plate, which allow rotation about the edges, but prevent displacement parallel to the edges and force the edges to remain straight. The two long edges are simply supported by struts, integral with the plate, which allow rotation about the edges, allow displacement parallel to the edges corresponding to the shortening of the strut under load, but maintain the edges in a straight line. The panel and struts transfer a shear load Q shown in figure 1.

The fundamental equations governing the deformation of thin plates were developed by Von Karman. They are (see reference 2, pp. 322-323):

$$\frac{\partial^4 F}{\partial x^4} + 2 \frac{\partial^4 F}{\partial x^2 \partial y^2} + \frac{\partial^4 F}{\partial y^4} = E \left[\left(\frac{\partial^2 w}{\partial x \partial y} \right)^2 - \frac{\partial^2 w}{\partial x^2} \frac{\partial^2 w}{\partial y^2} \right] \quad (1)$$

$$\frac{\partial^4 w}{\partial x^4} + 2 \frac{\partial^4 w}{\partial x^2 \partial y^2} + \frac{\partial^4 w}{\partial y^4} = \frac{p}{D} + \frac{h}{D} \left(\frac{\partial^2 F}{\partial y^2} - \frac{\partial^2 w}{\partial x^2} \right. \\ \left. + \frac{\partial^2 F}{\partial x^2 \partial y^2} - 2 \frac{\partial^2 F}{\partial x \partial y} \frac{\partial^2 w}{\partial x \partial y} \right) \quad (2)$$

where the median-fiber stresses are

$$\sigma_x' = \frac{\partial^2 F}{\partial y^2}; \quad \sigma_y' = \frac{\partial^2 F}{\partial x^2}; \quad \tau_{xy}' = -\frac{\partial^2 F}{\partial x \partial y} \quad (3)$$

and the median fiber strains are

$$\left. \begin{aligned} \epsilon_x' &= \frac{1}{E} \left(\frac{\partial^2 F}{\partial y^2} - \mu \frac{\partial^2 F}{\partial x^2} \right) \\ \epsilon_y' &= \frac{1}{E} \left(\frac{\partial^2 F}{\partial x^2} - \mu \frac{\partial^2 F}{\partial y^2} \right) \\ \gamma_{xy}' &= -\frac{2}{E} (1 + \mu) \frac{\partial^2 F}{\partial x \partial y} \end{aligned} \right\} \quad (4)$$

The extreme fiber bending stresses are

$$\left. \begin{aligned} \sigma_x'' &= -\frac{Eh}{2(1 - \mu^2)} \left(\frac{\partial^2 w}{\partial x^2} + \mu \frac{\partial^2 w}{\partial y^2} \right) \\ \sigma_y'' &= -\frac{Eh}{2(1 - \mu^2)} \left(\frac{\partial^2 w}{\partial y^2} + \mu \frac{\partial^2 w}{\partial x^2} \right) \\ \tau_{xy}'' &= -\frac{Eh}{2(1 + \mu)} \frac{\partial^2 w}{\partial x \partial y} \end{aligned} \right\} \quad (5)$$

Buckling Load

The theory for determining the buckling load of a simply supported rectangular plate under shear loads is given by Timoshenko on pages 357 to 360 of reference 2. This theory was worked out in detail for the case of a rectangular plate (fig. 1b) height-width ratio 2.5 in order to determine how many terms of the deflection equation

$$w = \sum_{m=1}^{\infty} \sum_{n=1}^{\infty} w_{m,n} \sin \frac{m\pi x}{a} \sin \frac{n\pi y}{b} \quad (6)$$

would be needed to give the buckling load with a negligible error.

If the 14 terms corresponding to $w_{1,2}$, $w_{1,4}$, $w_{1,6}$, $w_{2,1}$, $w_{2,3}$, $w_{2,5}$, $w_{2,7}$, $w_{3,2}$, $w_{3,4}$, $w_{3,6}$, $w_{4,1}$, $w_{4,3}$, $w_{4,5}$, $w_{4,7}$ ¹ and the theory of reference 2 are used, the buckling stress is

$$\tau = 5.554 \frac{Eh^2}{a^2}$$

If the eight terms $w_{1,2}$, $w_{1,4}$, $w_{1,6}$, $w_{2,1}$, $w_{2,3}$, $w_{2,5}$, $w_{3,2}$, $w_{3,4}$ are used, the buckling stress is

$$\tau = 5.555 \frac{Eh^2}{a^2}$$

If the seven terms $w_{1,2}$, $w_{1,4}$, $w_{2,1}$, $w_{2,3}$, $w_{2,5}$, $w_{3,2}$, $w_{3,4}$ are used

$$\tau = 5.567 \frac{Eh^2}{a^2}$$

If the six terms $w_{1,2}$, $w_{1,4}$, $w_{2,1}$, $w_{2,3}$, $w_{2,5}$, $w_{3,4}$ are used

$$\tau = 5.757 \frac{Eh^2}{a^2}$$

If the five terms $w_{1,2}$, $w_{1,4}$, $w_{2,1}$, $w_{2,3}$, $w_{2,5}$ are used

$$\tau = 5.823 \frac{Eh^2}{a^2}$$

¹It will be noted that the computation is confined to the deflection coefficients for which $m + n$ is an odd number, while Timoshenko confines his computation to the coefficients for which $m + n$ is an even number. Preliminary computation showed that Timoshenko's selection of coefficients gave the lower buckling load for a square plate while the present selection gave a lower buckling load for a plate with $b/a = 2.5$. The reason for this is obvious after considering probable buckling modes for plates with $b/a = 1$ and $b/a = 2.5$.

If the four terms $w_{1,2}$, $w_{1,4}$, $w_{2,1}$, $w_{2,3}$ are used

$$\tau = 5.867 \frac{Eh^2}{a^3}$$

It seems probable that the buckling stress with an unlimited number of terms would not differ appreciably from $5.554 \frac{Eh^2}{a^3}$. In the following work it will be assumed that the shape of the buckle is adequately described by limiting the summation in equation (6) to the 14 terms $w_{1,2}$, $w_{1,4}$, $w_{1,6}$, $w_{2,1}$, $w_{2,3}$, $w_{2,5}$, $w_{2,7}$, $w_{3,2}$, $w_{3,4}$, $w_{3,6}$, $w_{4,1}$, $w_{4,3}$, $w_{4,5}$, $w_{4,7}$.

At the start of buckling, the relative magnitude of the different terms is such that $w_{1,4}$, $w_{2,1}$, and $w_{2,3}$ are approximately $1/4$ of $w_{1,2}$; $w_{1,6}$, $w_{3,2}$, and $w_{3,4}$ are approximately $1/30$ of $w_{1,2}$; and the remaining terms are less than $1/100$ of $w_{1,2}$. It will be assumed in the following work that all products of $w_{m,n}$ coefficients can be neglected except those involving $w_{1,2}$, $w_{1,4}$, $w_{2,1}$, $w_{2,3}$.

Equilibrium of Median Fiber Forces

A suitable stress function, F , must now be chosen to satisfy equation (1), which expresses the condition that the median fiber forces are in equilibrium in the plane of the web. If F is taken as,

$$\begin{aligned}
F = & \frac{\bar{\sigma}_x y^2}{2} + \frac{\bar{\sigma}_y x^2}{2} - \tau x y + \sum_{m=0}^4 \sum_{n=0}^8 b_{m,n} \cos \frac{m\pi x}{a} \cos \frac{n\pi y}{b} \\
& + \sum_{m=2,4} A_m \cos \frac{m\pi x}{a} \left[\left(\frac{1-\mu}{1+\mu} - \frac{m\pi b}{2a} \coth \frac{m\pi b}{2a} \right) \cosh m\pi \left(\frac{y}{a} - \frac{b}{2a} \right) \right. \\
& \quad \left. + m\pi \left(\frac{y}{a} - \frac{b}{2a} \right) \sinh m\pi \left(\frac{y}{a} - \frac{b}{2a} \right) \right] \\
& + \sum_{m=1,3} A_m \cos \frac{m\pi x}{a} \left[\left(\frac{1-\mu}{1+\mu} - \frac{m\pi b}{2a} \tanh \frac{m\pi b}{2a} \right) \sinh m\pi \left(\frac{y}{a} - \frac{b}{2a} \right) \right. \\
& \quad \left. + m\pi \left(\frac{y}{a} - \frac{b}{2a} \right) \cosh m\pi \left(\frac{y}{a} - \frac{b}{2a} \right) \right] \\
& + \sum_{n=2,4,6,8} B_n \cos \frac{n\pi y}{b} \left[\left(\frac{1-\mu}{1+\mu} - \frac{n\pi a}{2b} \coth \frac{n\pi a}{2b} \right) \cosh n\pi \left(\frac{x}{b} - \frac{a}{2b} \right) \right. \\
& \quad \left. + n\pi \left(\frac{x}{b} - \frac{a}{2b} \right) \sinh n\pi \left(\frac{x}{b} - \frac{a}{2b} \right) \right] \\
& + \sum_{n=1,3,5,7} B_n \cos \frac{n\pi y}{b} \left[\left(\frac{1-\mu}{1+\mu} - \frac{n\pi a}{2b} \tanh \frac{n\pi a}{2b} \right) \sinh n\pi \left(\frac{x}{b} - \frac{a}{2b} \right) \right. \\
& \quad \left. + n\pi \left(\frac{x}{b} - \frac{a}{2b} \right) \cosh n\pi \left(\frac{x}{b} - \frac{a}{2b} \right) \right] \quad (7)
\end{aligned}$$

and if equations (6) and (7) are substituted into equation (1) with only products of $w_{1,2}$, $w_{2,1}$, $w_{3,2}$, and $w_{1,4}$ retained, it is found by a method shown in reference 3 that equation (1) is satisfied when

$$b_{0,0} = 0$$

$$b_{0,2} = \frac{E}{10.24} (-4w_{1,2}w_{1,4} + 8w_{2,1}^2 - 16w_{2,1}w_{2,3})$$

$$b_{0,4} = \frac{E}{163.8} (64w_{2,1}w_{2,3} + 8w_{1,2}^2)$$

$$b_{0,6} = \frac{E}{829.4} (36w_{1,2}w_{1,4} + 72w_{2,3}^2)$$

$$b_{0,8} = \frac{E}{2621} (32w_{1,4}^2)$$

$$b_{1,1} = \frac{E}{33.64} (-9w_{1,2}w_{2,1} - w_{1,2}w_{2,3} - 25w_{1,4}w_{2,3})$$

$$b_{1,3} = \frac{E}{148.8} (25w_{1,2}w_{2,1} - 49w_{1,4}w_{2,1})$$

$$b_{1,5} = \frac{E}{625.0} (49w_{1,2}w_{2,3} + 81w_{1,4}w_{2,1})$$

$$b_{1,7} = \frac{E}{1954} (121w_{1,4}w_{2,3})$$

$$b_{2,0} = \frac{E}{400} (8w_{1,2}^2 + 32w_{1,4}^2)$$

$$b_{2,2} = \frac{E}{538.2} (36w_{1,2}w_{1,4})$$

$$b_{2,4} = 0$$

$$b_{2,6} = \frac{E}{2381} (-4w_{1,2}w_{1,4})$$

$$b_{2,8} = 0$$

$$b_{3,1} = \frac{E}{3098} (25w_{1,2}w_{2,1} + 49w_{1,2}w_{2,3} + 121w_{1,4}w_{2,3})$$

$$b_{3,3} = \frac{E}{2725} (-9w_{1,2}w_{2,1} + 81w_{1,4}w_{2,1})$$

$$b_{3,5} = \frac{E}{4225} (-w_{1,2}w_{2,3} - 49w_{1,4}w_{2,1})$$

$$b_{3,7} = \frac{E}{7090} (-25w_{1,4}w_{2,3})$$

$$b_{4,0} = \frac{E}{6400} (8w_{2,1}^2 + 72w_{2,3}^2)$$

$$b_{4,2} = \frac{E}{6922} (64w_{2,1}w_{2,3})$$

$$b_{4,4} = \frac{E}{8612} (-16w_{2,1}w_{2,3})$$

$$b_{4,6} = 0; \quad b_{4,8} = 0$$

$b_{m,n} = 0$ whenever $m + n$ is an odd number

(8)

Boundary Conditions

The condition that the edges of the plate be simply supported is automatically satisfied by equation (6) for the lateral deflection.

The condition that the edges of the plate act integrally with the supporting struts and flanges of the beam requires that the strain at the edge of the plate be equal to the strain in the supporting strut or flange. This condition will be used to determine the remaining coefficients \bar{G}_x , \bar{G}_y , A_m , B_n in equation (7).

The edges $y = 0$, $y = b$ (see fig 1b) are considered to be supported by flanges so heavy that they do not shorten under load. The median fiber strain in the x-direction at the edges $y = 0$, $y = b$ must, therefore, be zero,

$$(\epsilon_x')_{y=0, y=b} = 0 \quad (9)$$

The edges $x=0$, $x=a$ are considered to be supported by struts having $1/4$ the area of the sheet, that is, $ah/4$. If the compressive force in the strut is denoted by P (P is a function of y), the median fiber strain in the y-direction at the edges $x=0$, $x=a$ must be,

$$(\epsilon_y')_{x=0, x=a} = - \frac{4P}{ahE} \quad (10)$$

Since there are an equal number of web bays and struts in the middle portion of the beam, the compressive force in a strut must equal the vertical tensile force in a web bay, or

$$P = \int_0^a h \sigma_y' dx \quad (11)$$

Substituting from equations (3) and (7) into equation (11) and performing the indicated integration gives,

$$P = ah \bar{\sigma}_y + \frac{4\pi h}{b(1+\mu)} \sum_{n=2}^8 nB_n \sinh \frac{n\pi a}{2b} \cos \frac{n\pi y}{b} \quad (12)$$

Substituting equation (12) into equation (10) gives

$$(\epsilon_y^1)_{x=0, x=a} = -\frac{4}{E} \bar{\sigma}_y - \frac{16\pi}{abE(1+\mu)} \sum_{n=2}^8 nB_n \sinh \frac{n\pi a}{2b} \cos \frac{n\pi y}{b} \quad (13)$$

The fact that the summations in the series expansion for F , equation (7), have been limited to $m = 4$ and $n = 8$ makes it impossible to satisfy the boundary equations (9) and (13) identically. Except for a small variation in strain of a frequency higher than the fourth harmonic in x and eighth harmonic in y , however, it can be shown by expanding F into trigonometric series and by substituting equations (4), (7), and (8) into equations (9) and (13) that equations (9) and (13) are satisfied when,

$$\begin{aligned}
 \bar{\sigma}_y &= \frac{E}{a^2} (0.2408w_{1,2}^2 + 0.7242w_{1,4}^2 + 0.3588w_{2,1}^2 + 0.6810w_{2,3}^2) \\
 \bar{\sigma}_x &= \frac{E}{a^2} (1.310w_{1,2}^2 + 1.463w_{1,4}^2 + 5.048w_{2,1}^2 + 5.150w_{2,3}^2) \\
 A_1 &= \frac{E}{10^8} (-0.2743w_{1,2}w_{2,1} - 0.5940w_{1,2}w_{2,3} - 0.1770w_{1,4}w_{2,1} \\
 &\quad - 0.7598w_{1,4}w_{2,3}) \\
 B_1 &= \frac{E}{10^8} (34.26w_{1,2}w_{2,1} - 51.47w_{1,2}w_{2,3} - 1.758w_{1,4}w_{2,1} + 39.99w_{1,4}w_{2,3}) \\
 A_2 &= \frac{E}{10^7} (-21.46w_{1,2}^2 - 75.92w_{1,4}^2 - 7.900w_{2,1}^2 - 9.409w_{2,3}^2 \\
 &\quad - 24.46w_{1,2}w_{1,4} - 2.159w_{2,1}w_{2,3}) \\
 B_2 &= \frac{E}{10^5} (-0.1173w_{1,2}^2 - 0.4122w_{1,4}^2 - 20.84w_{2,1}^2 - 0.09173w_{2,3}^2 \\
 &\quad + 43.67w_{1,2}w_{1,4} + 60.78w_{2,1}w_{2,3}) \\
 A_3 &= \frac{E}{10^6} (1.512w_{1,2}w_{2,1} + 2.523w_{1,2}w_{2,3} + 3.745w_{1,4}w_{2,1} + 11.56w_{1,4}w_{2,3}) \\
 B_3 &= \frac{E}{10^6} (-6.326w_{1,2}w_{2,1} - 3.566w_{1,2}w_{2,3} - 6.529w_{1,4}w_{2,1} - 4.368w_{1,4}w_{2,3}) \\
 A_4 &= \frac{E}{10^{12}} (-15.97w_{1,2}^2 - 25.70w_{1,4}^2 - 68.87w_{2,1}^2 - 472.8w_{2,3}^2 \\
 &\quad + 9.950w_{1,2}w_{1,4} - 306.7w_{2,1}w_{2,3}) \\
 B_4 &= \frac{E}{10^5} (-52.13w_{1,2}^2 - 7.940w_{1,4}^2 - 1.003w_{2,1}^2 - 2.237w_{2,3}^2 \\
 &\quad - 2.510w_{1,2}w_{1,4} - 435.6w_{2,1}w_{2,3}) \\
 B_5 &= \frac{E}{10^5} (-11.24w_{1,2}w_{2,1} - 6.647w_{1,2}w_{2,3} + 92.90w_{1,4}w_{2,1} - 27.83w_{1,4}w_{2,3}) \\
 B_6 &= \frac{E}{10^5} (-3.450w_{1,2}^2 - 12.01w_{1,4}^2 - 1.677w_{2,1}^2 - 299.7w_{2,3}^2 \\
 &\quad - 158.2w_{1,2}w_{1,4} - 2.320w_{2,1}w_{2,3}) \\
 B_7 &= \frac{E}{10^5} (-9.777w_{1,2}w_{2,1} - 21.75w_{1,2}w_{2,3} - 4.193w_{1,4}w_{2,1} + 112.33w_{1,4}w_{2,3}) \\
 B_8 &= \frac{E}{10^7} (-5.152w_{1,2}^2 - 148.0w_{1,4}^2 - 2.775w_{2,1}^2 - 8.755w_{2,3}^2 \\
 &\quad - 5.482w_{1,2}w_{1,4} - 4.772w_{2,1}w_{2,3})
 \end{aligned}
 \tag{14}$$

The struts and flanges are considered to be stiff enough in bending to keep straight the four edges ($x=0$, $x=a$, $y=0$, $y=b$) of the plate. Equations for the u and v displacements, in the x and y directions, respectively, can be obtained from page 322 of reference 2.

$$\left. \begin{aligned} \frac{\partial u}{\partial x} &= \epsilon_x' - \frac{1}{2} \left(\frac{\partial w}{\partial x} \right)^2 \\ \frac{\partial v}{\partial y} &= \epsilon_y' - \frac{1}{2} \left(\frac{\partial w}{\partial y} \right)^2 \\ \frac{\partial u}{\partial y} + \frac{\partial v}{\partial x} &= \gamma_{xy}' - \frac{\partial w}{\partial x} \frac{\partial w}{\partial y} \end{aligned} \right\} \quad (15)$$

Values of u and v can be obtained by substituting equations (4), (6), (7), (8), and (14) into equations (15) and integrating. This gives for the values of u and v at the edges of the plate

$$\left. \begin{aligned} (u)_{x=0} &= 0; \quad (u)_{x=a} = 0 \\ (v)_{y=0} &= 2.632 \tau x/B \\ (v)_{y=b} &= 2.632 \tau x/B - \frac{4}{b} \left(1.504 w_{1,2}^2 + 4.535 w_{1,4}^2 \right. \\ &\quad \left. + 2.242 w_{2,1}^2 + 4.257 w_{2,3}^2 \right) \end{aligned} \right\} \quad (16)$$

It is seen from equations (16) that the edges of the plate, corresponding to $x=0$, $x=a$, $y=0$, $y=b$, satisfy the condition of remaining straight after buckling has started.

Equilibrium of Lateral Forces

Equation (2) expresses the equilibrium between the components of the membrane forces in a direction perpendicular to the plate and the opposing forces developed by the plate because of its flexural rigidity. The fact that the series

expression for w , equation (6), has been limited to 14 terms and the fact that only those square and cubic products involving the 4 biggest terms in w are considered, make it impossible to satisfy equation (2) identically. Except for small unequilibrated lateral pressures of high order, however, it can be shown by expanding F into trigonometric series and by substituting equations (6), (7), (8), and (14) into (2) as is done in reference 3, that equation (2) is satisfied when the equations in table 1 are satisfied. As an example of the use of this table, the first equation is

$$0 = 24.26w_{1,2}h^2 + 5.689w_{2,1}\tau a^2/E - 10.24w_{2,3}\tau a^2/E - 4.063w_{2,5}\tau a^2/E \dots + 23.13w_{1,2}^3 + 0.04156w_{1,2}^2w_{1,4} + \dots \quad (17)$$

Shear Load Carried by Beam

The beam (fig. 1a) supports a shear load Q . At any vertical section through the beam this load is partially carried by shear in the web and partially by shear in the flanges. Part of the shear in the web may be considered as due to the diagonal tension after buckling.

Making use of the fact that the flange bending moment is the same at each strut point, the shearing force in the upper flange is

$$\int_x^a h(\sigma_y')_{y=b} dx - \frac{1}{a} \int_0^a h(\sigma_y')_{y=b} x dx \quad (18)$$

and in the lower flange is

$$\frac{1}{a} \int_0^a h(\sigma_y')_{y=0} x dx - \int_x^a h(\sigma_y')_{y=0} dx \quad (19)$$

where the shearing force in either flange is considered positive if it tends to support the external load Q directed as shown in figure 1a. The shear load carried by the web is

$$- \int_0^b h \tau_{xy'} dy \quad (20)$$

Adding equations (18), (19), and (20), substituting for σ_y' and τ_{xy}' their values as given by equations (3), (7), (8), and (14), and integrating gives

$$Q = -\tau_{bh} + \frac{Eh}{a} \left(-1.352w_{1,2}w_{2,1} + 2.427w_{1,2}w_{2,3} - 0.5406w_{1,4}w_{2,1} - 3.474w_{1,4}w_{2,3} \right) \quad (21)$$

Shearing Deformation of Beam

The shearing forces acting on the end of the beam cause it to shear downward as shown in figure 1a. The amount of the downward displacement is given by equation (16) as:

$$(v)_{y=0} = 2.632 \frac{\tau x}{E} = \bar{Y}x; \quad \bar{Y} = 2.632 \frac{\tau}{E} \quad (22)$$

where \bar{Y} is the shear deformation of the beam.

Effective Width in Shear

The loss in shear stiffness of the beam after buckling may be considered as a loss in effective width of the sheet. Define the effective width ratio in shear for a given shearing deformation \bar{Y} as the ratio of the load Q actually carried to the load τ_{bh} which would have been carried in the absence of buckling. The effective width ratio is, therefore,

$$\text{Effective width ratio} = Q/(-\tau_{bh}) \quad (23)$$

Substituting the value of Q given in equation (21) and $b = 2.5a$ gives

$$\begin{aligned} \text{Effective width ratio} &= 1 - \frac{E}{\tau a^2} \left(-0.5408w_{1,2}w_{2,1} \right. \\ &\quad \left. + 0.9708w_{1,2}w_{2,3} - 0.2162w_{1,4}w_{2,1} - 1.390w_{1,4}w_{2,3} \right) \quad (24) \end{aligned}$$

Compressive Force in Vertical Strut

After buckling of the web, the diagonal tension field tends to draw the flanges of the beam together. This action is resisted by the vertical struts. The magnitude of the resulting compressive force P in the strut is given by equation (12). Substituting for $\bar{\sigma}_y$, B_2 , B_4 , B_6 , and B_8 the values given in equation (14) gives

$$\begin{aligned}
 P = \frac{Eh}{a} & \left\{ \left(0.2408w_{1,a}^2 + 0.7242w_{1,4}^2 + 0.3588w_{2,1}^2 + 0.681w_{2,3}^2 \right) \right. \\
 & + \cos \frac{2\pi y}{b} \left(-0.00145w_{1,2}^2 - 0.00508w_{1,4}^2 - 0.257w_{2,1}^2 \right. \\
 & \quad \left. \left. - 0.00113w_{2,3}^2 + 0.539w_{1,2}w_{1,4} + 0.750w_{2,1}w_{2,3} \right) \right. \\
 & + \cos \frac{4\pi y}{b} \left(-0.0488w_{1,2}^2 - 0.00744w_{1,4}^2 - 0.00094w_{2,1}^2 \right. \\
 & \quad \left. \left. - 0.00209w_{2,3}^2 - 0.00235w_{1,2}w_{1,4} - 0.408w_{2,1}w_{2,3} \right) \right. \\
 & + \cos \frac{6\pi y}{b} \left(-0.00171w_{1,2}^2 - 0.00597w_{1,4}^2 - 0.0083w_{2,1}^2 \right. \\
 & \quad \left. \left. - 0.1489w_{2,3}^2 - 0.0786w_{1,2}w_{1,4} - 0.00015w_{2,1}w_{2,3} \right) \right. \\
 & + \cos \frac{8\pi y}{b} \left(-0.00120w_{1,2}^2 - 0.0345w_{1,4}^2 - 0.00065w_{2,1}^2 \right. \\
 & \quad \left. \left. - 0.00204w_{2,3}^2 - 0.00128w_{1,2}w_{1,4} - 0.00111w_{2,1}w_{2,3} \right) \right\} \\
 & \quad (25)
 \end{aligned}$$

Stress at Center of Shear Bay

The median fiber stress at the center of the plate is obtained from equations (3), (7), (8), and (14) by letting $x = a/2$, $y = b/2$. This gives

$$\left. \begin{aligned}
 (\sigma_x')_{\substack{x=a/2 \\ y=b/2}} &= \frac{E}{a^2} \left(0.04978w_{1,2}^2 + 0.2200w_{1,4}^2 + 10.11w_{2,1}^2 \right. \\
 &\quad \left. + 10.14w_{2,3}^2 - 0.5638w_{1,2}w_{1,4} - 20.23w_{2,1}w_{2,3} \right) \\
 (\sigma_y')_{\substack{x=a/2 \\ y=b/2}} &= \frac{E}{a^2} \left(1.032w_{1,2}^2 + 3.890w_{1,4}^2 + 0.2986w_{2,1}^2 \right. \\
 &\quad \left. - 1.116w_{2,3}^2 - 2.872w_{1,2}w_{1,4} + 1.357w_{2,1}w_{2,3} \right) \\
 (\tau_{xy}')_{\substack{x=a/2 \\ y=b/2}} &= \tau - \frac{E}{a^2} \left(-5.306w_{1,2}w_{2,1} + 1.954w_{1,2}w_{2,3} \right. \\
 &\quad \left. + 8.223w_{1,4}w_{2,1} - 6.549w_{1,4}w_{2,3} \right)
 \end{aligned} \right\} \quad (26)$$

The bending stress at the center of the plate is obtained by substituting equation (6) into equations (5) with $x=a/2$, $y=b/2$. This gives

$$\left. \begin{aligned}
 (\sigma_x'')_{\substack{x=a/2 \\ y=b/2}} &= 5.482(\frac{Eh}{a^2}) \sum_{m,n} w_{m,n} (m^2 + 0.05060n^2) \sin \frac{m\pi}{2} \sin \frac{n\pi}{2} \\
 (\sigma_y'')_{\substack{x=a/2 \\ y=b/2}} &= 5.482(\frac{Eh}{a^2}) \sum_{m,n} w_{m,n} (0.16n^2 + 0.316m^2) \sin \frac{m\pi}{2} \sin \frac{n\pi}{2} \\
 (\tau_{xy}'')_{\substack{x=a/2 \\ y=b/2}} &= -1.500(\frac{Eh}{a^2}) \sum_{m,n} mn w_{m,n} \cos \frac{m\pi}{2} \cos \frac{n\pi}{2}
 \end{aligned} \right\} \quad (27)$$

The equations (27) show that all the bending stresses are zero in the present problem. This result can be derived also by direct inspection of (6), noting that $m + n$ is odd and that consequently the point $x=a/2$, $y=b/2$ must lie on a nodal line.

Stress at Corner of Shear Bay

The membrane stress at the upper corner of the plate $x=0, y=b$, toward which the diagonal tension buckle points is obtained by substituting equations (7), (8), and (14) into equation (3). This gives

$$\begin{aligned}
 (\sigma_x')_{\substack{x=0 \\ y=b}} &= \frac{E}{a^2} \left(-0.1801w_{1,2}^2 - 0.7100w_{1,4}^2 - 0.0491w_{2,1}^2 \right. \\
 &\quad - 0.3361w_{2,3}^2 - 0.5827w_{1,2}w_{1,4} - 0.2146w_{2,1}w_{2,3} \\
 &\quad + 0.197w_{1,2}w_{2,1} + 0.561w_{1,2}w_{2,3} - 0.1613w_{1,4}w_{2,1} \\
 &\quad \left. - 0.2033w_{1,4}w_{2,3} \right) \\
 (\sigma_y')_{\substack{x=0 \\ y=b}} &= \frac{E}{a^2} \left(-0.7124w_{1,2}^2 - 2.592w_{1,4}^2 - 0.1627w_{2,1}^2 \right. \\
 &\quad - 1.899w_{2,3}^2 - 1.918w_{1,2}w_{1,4} - 1.233w_{2,1}w_{2,3} \\
 &\quad + 0.3037w_{1,2}w_{2,1} + 0.7445w_{1,2}w_{2,3} - 0.0644w_{1,4}w_{2,1} \\
 &\quad \left. + 0.1524w_{1,4}w_{2,3} \right) \\
 (\tau_{xy}')_{\substack{x=0 \\ y=b}} &= \tau
 \end{aligned} \tag{28}$$

The bending stress at the corner of the plate is obtained by substituting equation (6) into equations (5) with $x=0, y=b$. This gives zero for σ_x'' and σ_y'' at $x=0, y=b$ and

$$(\tau_{xy}'')_{x=0, y=b} = -1.500(Eh/a^2) \sum_m \sum_n m n w_{m,n} \cos n\pi \tag{29}$$

Principal Stresses

The maximum and minimum principal stresses may be determined from the stresses σ_x , σ_y , and τ_{xy} by the equations on page 19 of reference 4

$$\left. \begin{aligned} \sigma_{\max} &= \frac{\sigma_x + \sigma_y}{2} + \sqrt{\left(\frac{\sigma_x - \sigma_y}{2}\right)^2 + \tau_{xy}^2} \\ \tan 2a &= 2 \frac{\tau_{xy}}{\sigma_x - \sigma_y} \end{aligned} \right\} \quad (30)$$

where a is the angle between the x -axis and the direction of a principal stress.

NUMERICAL SOLUTION

Deflection Coefficients

The deflection coefficients are obtained by solution of the simultaneous equations in table 1, such as equation (17). These equations were solved for values $Q < 7.44 \text{ Eh}^3 b/a^2$ by a method of successive approximation, using the following steps:

1. Divide each equation by h^3 .
2. Estimate values of $\tau a^2/Eh^2$, $w_{1,4}/h$, $w_{1,6}/h$, $w_{2,1}/h$, $w_{2,3}/h$, $w_{2,5}/h$, $w_{2,7}/h$, $w_{3,2}/h$, $w_{3,4}/h$, $w_{3,6}/h$, $w_{4,1}/h$, $w_{4,3}/h$, $w_{4,5}/h$, and $w_{4,7}/h$, corresponding to a given value of $w_{1,2}/h$.
3. Expand the right-hand side of each of the first four equations in a Taylor series in $\tau a^2/Eh^2$ in $w_{1,4}/h$, $w_{2,1}/h$, $w_{2,3}/h$, in the neighborhood of the estimated values, retaining all the deflection coefficients in determining the constant term.
4. Solve the resulting four linear equations for the difference between the chosen values of $\tau a^2/Eh^2$, $w_{1,4}/h$,

$w_{2,1}/h$, $w_{2,3}/h$ and the improved values. (Crout's method, (reference 5) was used for this.)

5. Substitute these improved values into the remaining equations of table 1 and solve for the remaining deflection coefficients by successive approximation.

6. Repeat, using the improved values as an initial estimate until the estimated error is less than 1/2 percent.

The convergence of this method was slow because of the large number of variables involved. In order to improve the convergence for values of $Q > 7.44 Eh^3 b/a^2$ the smaller deflection coefficients were approximated by the ratios of their values at $Q = 7.44 Eh^3 b/a^2$ by taking $w_{1,6} = 0.424w_{3,2}$, $w_{2,5} = -0.189w_{3,2}$, $w_{2,7} = -0.087w_{3,2}$, $w_{3,4} = -0.872w_{3,2}$, $w_{3,6} = -0.164w_{3,2}$, $w_{4,1} = -0.054w_{3,2}$, $w_{4,3} = 0.039w_{3,2}$, $w_{4,5} = 0.033w_{3,2}$, $w_{4,7} = 0.027w_{3,2}$ and proceeding as before except for including the first five equations of table 1 in steps 3 and 4 and determining the remaining deflection coefficients from the above linear relations rather than from step 5. The convergence using this method was rapid; one or two trials usually were sufficient to give an accurate answer.

The results are given table 2 for values of the shear load Q up to about four times the critical value for buckling. The value of \bar{Y} was computed from τ by using equation (22); Q was computed from τ , $w_{1,2}$, $w_{1,4}$, $w_{2,1}$, and $w_{2,3}$ by using equation (21).

Median Fiber Stresses at Center of Shear Web

The median fiber stresses at the center of the shear web were computed from equations (26) and table 2. The bending stresses at the center of the plate were seen to be zero from equation (27). The maximum and minimum principal stresses were then computed from equation (30). These stresses are given in table 3 and are plotted against the shear load Q in dimensionless form in figure 2.

As might be expected, the maximum principal stress (corresponding to tension along the wrinkles) continues to rise after buckling, while the minimum principal stress (corresponding to compression across the wrinkles), decreases slowly

after buckling at $Q = 5.54 Eh^3 b/a^2$. The direction of the maximum principal stress forms an angle of 45° with the flanges at the buckling load; however, this angle drops to $32^\circ 34'$ at the highest load considered.

Stresses at Corner of Shear Web

The stresses at the upper corner of the shear web toward which the wrinkles point ($x=0, y=b$) were computed from equations (28) and (29) and table 2. The maximum and minimum principal median fiber stresses were then computed from equation (30). These stresses are given in table 4 and some of them are plotted against load Q in dimensionless form in figure 3.

Figure 3 shows that in the corner of the shear web, the minimum median fiber stress (compression) is about 30 percent larger in absolute value than the maximum median fiber stress (tension). This is in sharp contrast to the condition at the center of the shear web (fig. 2) where the tension is much larger than the compression. The bending stress at the corner (fig. 3) is about half as large as the median fiber stresses. The angle of the maximum median fiber stress in the corner (fig. 3) changes from 45° at buckling to about 43° at the highest load considered. This is a much smaller change in angle than was found in the center of the bay (fig. 2).

Shear Deformation of Beam

The shear deformation \bar{Y} of the beam and the shear load Q are given in dimensionless form in table 2. They are plotted against each other in figure 4. It is seen from this figure that the break in the deformation-load curve at the buckling load, $Q = 5.54 Eh^3 b/a^2$ is not very sharp. The stiffness, as indicated by the reciprocal of the slope of the deformation-load curve, shows a drop of about 15 percent after buckling.

Effective Width of Sheet

The effective width of the sheet, corresponding to the width of unbuckled sheet which would give the same shear deformation as the actual buckled sheet, was computed from equation (24) and table 2. The ratio of effective to initial width is given in table 4 and is plotted in figure 5 against

the shear deformation ratio $-\bar{Y}a^2/h^2$. Figure 5 shows that the effective width decreases slowly with increase in shear deformation. At the maximum deformation considered, about five times the deformation at the instant of buckling, the effective width is still about 86 percent of the initial width.

Compressive Force in Strut

The distribution of compressive force P along the strut was computed from equation (12), using equation (14) and table 2. The results are plotted in dimensionless form in figure 6 for $Q = 9.30 \frac{Eh^3b}{a^2}$. The variation in compressive force, P , along the strut is quite pronounced, the force being more than three times as large at the center as at the ends. This is a much larger variation than was found in reference 1 for a square shear web.

The maximum force $P_{y=b/2}$ was computed for various loads and is plotted in dimensionless form in figure 7 as a function of load Q . The increase in strut force with load is nearly linear after buckling at $Q = 5.54 \frac{Eh^3b}{a^2}$.

Comparison with Results for Shear Web Having Square Bays (Reference 1)

The above results for a 2.5:1 rectangular shear web with reinforcement ratio 1/4, are compared in figures 8, 9, and 10 with the corresponding results given in reference 1 for a square shear web with the same reinforcement ratio. Curves A are taken from the present analysis, while curves B are taken from reference 1. Figure 8 shows that the difference in shear deformation for the deep web and for the square web does not exceed 2 percent. Figure 9 shows that the difference in stresses at the corners in line with the diagonal tension wrinkles (subscript 2) does not exceed 10 percent, while the stresses at the center of the deep web (subscript 1) are up to 20 percent smaller than those for the square web. Figure 10 shows that the force at the center of the strut reinforcing the deep web is about 30 percent greater at the highest load than that for the square web.

Comparison with "Tension Field" Theory

The curves C in figures 8 to 10 were computed from Kuhn's semiempirical analysis of shear webs in incomplete diagonal tension (reference 6). The shear deformation (fig. 8) is about 10 percent greater by Kuhn's analysis than by the present analysis; the median fiber tension at the center of the web bay (fig. 9) is up to 12 percent greater by Kuhn's analysis than by the present analysis; the median fiber tension at the corner of the web bay (fig. 9) is up to 37 percent greater by Kuhn's analysis than by the present analysis; and the force at the middle of the strut (fig. 10) is about 16 percent less by Kuhn's analysis than by the present analysis. The comparison indicates that Kuhn's analysis is more conservative than the present analysis except for strut force.

The curves D in figures 8 to 10 were computed from Langhaar's analysis (reference 7) which takes account of flange and strut stiffness, but neglects the effect of Poisson's ratio ($\mu = 0$). The shear deformation (fig. 8) is up to 80 percent greater by Langhaar's analysis than by the present analysis, the median fiber tension at the center of the web (fig. 9) is up to 50 percent greater by Langhaar's analysis than by the present analysis; the median fiber tension at the corners in line with the diagonal tension wrinkles is up to 90 percent greater by Langhaar's analysis than by the present analysis; and the force at the middle of the strut (fig. 10) is about four times as great at the highest load. The comparison indicates that Langhaar's analysis is more conservative by a large margin than the present analysis.

CONCLUSIONS

The analysis of a rectangular shear web with a height-to-width ratio 2.5 reinforced by struts with a weight equal to one-fourth the weight of the web leads to the following results.

The maximum principal stress at the center (corresponding to tension along the wrinkle) continues to rise after buckling, while the minimum principal stress (corresponding to compression perpendicular to the wrinkles) remains constant and then decreases slowly with increasing load. The direction of the maximum principal stress at the center forms an angle of 45° with the flanges at the buckling load; the angle decreases with increasing load; it is only about 32° at four times the buckling load.

In the corners of the web that are in line with the diagonal wrinkles, the minimum median fiber stress (compression) is about 30 percent larger in absolute value than the maximum median fiber stress (tension). This is in sharp contrast to the condition at the center of the shear web where the tension is much larger than the compression. The bending stress at the corner is about one-half as large as the median fiber stresses. The direction of the maximum median fiber stress in the corner changes from 45° relative to the flanges at buckling to about 43° at four times the buckling load.

The slope of the shear deformation - load curve shows an abrupt decrease in shear stiffness of about 15 percent at the buckling load.

The effective width of the sheet drops off slowly as the buckling load is exceeded. At a shear deformation of about five times the buckling deformation the effective width is still 86 percent of the initial width.

The compressive force in the strut is about three times as large at the middle as at the ends. This is a much larger variation than was found in reference 1 for a square shear web; it is probably caused by "gusset" action near the ends of the relatively longer struts reinforcing the rectangular web. The increase in strut force with load was roughly linear.

Comparison with the corresponding analysis of reference 1 for square shear bays shows agreement within 2 percent for shear deformation. The stresses at the center and corners and the force in the middle of the strut differed by not more than 30 percent.

Comparison with the diagonal tension field theory as developed by Kuhn indicates that Kuhn's analysis is up to 37 percent more conservative than the present analysis except for strut force, for which the present analysis is more conservative.

Comparison with the diagonal tension field theory as developed by Langhaar indicates that Langhaar's analysis is much more conservative than the present analysis; the difference is of the order of 50 to 400 percent at the largest loads.

REFERENCES

1. Levy, Samuel, Fienup, Kenneth L., and Woolley, Ruth M.: Analysis of Square Shear Web above Buckling Load. NACA TN No. 962, 1945.
2. Timoshenko, S.: Theory of Elastic Stability. McGraw-Hill Book Co., Inc., 1936.
3. Levy, Samuel: Bending of Rectangular Plates with Large Deflections. NACA Rep. No. 737, 1942. (Issued also as TN No. 846, 1942)
4. Timoshenko, S.: Theory of Elasticity. McGraw-Hill Book Co., Inc., 1934.
5. Crout, Prescott, D.: A Short Method for Evaluating Determinants and Solving Systems of Linear Equations with Real or Complex Coefficients. Trans. A.I.E.E., vol. 60, 1941, pp. 1235-1241.
6. Kuhn, Paul: Investigations on the Incompletely Developed Plane Diagonal-Tension Field. NACA Rep. No. 697, 1940.
7. Langhaar, H. L.: Theoretical and Experimental Investigations of Thin-Webbed Plate-Girder Beams. Trans. A.S.M.E., vol. 65, Oct. 1943, pp. 799-802.

TABLE 1 - EQUATIONS FOR DEFLECTION COEFFICIENTS
 [See Equation (17)]

	0=	0=	0=	0=	0=	0=	0=
$w_{1,2}$	$24.26h^2$	0	$5.689\frac{Ta^2}{E}$	$-10.24\frac{Ta^2}{E}$	0	$-4.063\frac{Ta^2}{E}$	$-2.654\frac{Ta^2}{E}$
$w_{1,4}$	0	$114.3h^2$	$2.276\frac{Ta^2}{E}$	$14.63\frac{Ta^2}{E}$	0	$-18.96\frac{Ta^2}{E}$	$-7.240\frac{Ta^2}{E}$
$w_{1,6}$	0	0	$1.463\frac{Ta^2}{E}$	$5.689\frac{Ta^2}{E}$	$412.2h^2$	$83.27\frac{Ta^2}{E}$	$-87.57\frac{Ta^2}{E}$
$w_{2,1}$	$5.689\frac{Ta^2}{E}$	$2.276\frac{Ta^2}{E}$	$156.1h^2$	0	$1.463\frac{Ta^2}{E}$	0	0
$w_{2,3}$	$-10.24\frac{Ta^2}{E}$	$14.63\frac{Ta^2}{E}$	0	$268.9h^2$	$5.689\frac{Ta^2}{E}$	0	0
$w_{2,5}$	$-4.063\frac{Ta^2}{E}$	$-18.96\frac{Ta^2}{E}$	0	0	$23.27\frac{Ta^2}{E}$	$577.2h^2$	0
$w_{2,7}$	$-2.655\frac{Ta^2}{E}$	$-7.240\frac{Ta^2}{E}$	0	0	$-27.57\frac{Ta^2}{E}$	0	$1284h^2$
$w_{3,2}$	0	0	$-10.24\frac{Ta^2}{E}$	$18.43\frac{Ta^2}{E}$	0	$7.314\frac{Ta^2}{E}$	$4.775\frac{Ta^2}{E}$
$w_{3,4}$	0	0	$-4.066\frac{Ta^2}{E}$	$-26.33\frac{Ta^2}{E}$	0	$34.13\frac{Ta^2}{E}$	$13.03\frac{Ta^2}{E}$
$w_{3,6}$	0	0	$-2.653\frac{Ta^2}{E}$	$-10.24\frac{Ta^2}{E}$	0	$-41.89\frac{Ta^2}{E}$	$49.62\frac{Ta^2}{E}$
$w_{4,1}$	$2.276\frac{Ta^2}{E}$	$.9102\frac{Ta^2}{E}$	0	0	$.5851\frac{Ta^2}{E}$	0	0
$w_{4,3}$	$-4.096\frac{Ta^2}{E}$	$5.851\frac{Ta^2}{E}$	0	0	$2.276\frac{Ta^2}{E}$	0	0
$w_{4,5}$	$-1.625\frac{Ta^2}{E}$	$-7.585\frac{Ta^2}{E}$	0	0	$9.309\frac{Ta^2}{E}$	0	0
$w_{4,7}$	$-1.082\frac{Ta^2}{E}$	$-2.698\frac{Ta^2}{E}$	0	0	$11.03\frac{Ta^2}{E}$	0	0
$w_{1,2}^2$	$23.13w_{1,2}$	$.01385w_{1,2}$	$85.22w_{2,1}$	$23.91w_{2,1}$	$-8.388w_{1,2}$	$-23.78w_{2,1}$	$-.1858w_{2,1}$
$w_{1,2}^2$	$.04156w_{1,4}$	$66.53w_{1,4}$	$23.91w_{2,3}$	$86.49w_{2,3}$	$44.32w_{1,4}$	$4.112w_{2,3}$	$-28.75w_{2,3}$
$w_{1,4}^2$	$.04907w_{1,4}$	$79.07w_{1,4}$	$175.8w_{2,1}$	$1.760w_{2,1}$	$.09244w_{1,4}$	$.9703w_{2,1}$	$65.44w_{2,1}$
$w_{1,4}^2$	$68.52w_{1,2}$	$.1472w_{1,2}$	$1.760w_{2,3}$	$213.1w_{2,3}$	$8.339w_{1,2}$	$72.56w_{2,3}$	$2.377w_{2,3}$
$w_{2,1}^2$	$85.22w_{1,2}$	$-58.27w_{1,2}$	$299.0w_{2,1}$	$-89.75w_{2,1}$	$-.3030w_{1,2}$	$-.000971w_{2,1}$	$-.002909w_{2,1}$
$w_{2,1}^2$	$-58.27w_{1,4}$	$175.8w_{1,4}$	$-299.2w_{2,3}$	$807.5w_{2,3}$	$-88.73w_{1,4}$	$-302.4w_{2,3}$	$-.007190w_{2,3}$
$w_{2,3}^2$	$86.49w_{1,2}$	$38.29w_{1,2}$	$.02106w_{2,3}$	$234.0w_{2,3}$	$-5.814w_{1,2}$	$.07389w_{2,3}$	$.01265w_{2,3}$
$w_{2,3}^2$	$36.28w_{1,4}$	$213.1w_{1,4}$	$607.5w_{2,1}$	$.06318w_{2,1}$	$-7.329w_{1,4}$	$316.0w_{2,1}$	$-305.1w_{2,1}$
$w_{1,2}w_{1,4}w_{2,1}$	0	0	-116.5	120.5	0	65.22	-60.97
$w_{1,2}w_{1,4}w_{2,3}$	0	0	120.5	72.58	0	122.1	1.262
$w_{1,2}w_{2,1}w_{2,3}$	47.82	120.5	0	0	-145.8	0	0
$w_{1,4}w_{2,1}w_{2,3}$	120.6	3.520	0	0	232.9	0	0

TABLE I (Continued)

	0-	0-	0-	0-	0-	0-	0-
$w_{1,2}$	0	0	0	$2.276 \frac{T^2}{E}$	$-4.096 \frac{T^2}{E}$	$-1.625 \frac{T^2}{E}$	$-1.062 \frac{T^2}{E}$
$w_{1,4}$	0	0	0	$.9102 \frac{T^2}{E}$	$5.851 \frac{T^2}{E}$	$-7.565 \frac{T^2}{E}$	$-2.896 \frac{T^2}{E}$
$w_{1,6}$	0	0	0	$.5851 \frac{T^2}{E}$	$2.276 \frac{T^2}{E}$	$9.309 \frac{T^2}{E}$	$-11.03 \frac{T^2}{E}$
$w_{2,1}$	$-10.24 \frac{T^2}{E}$	$-4.096 \frac{T^2}{E}$	$-2.633 \frac{T^2}{E}$	0	0	0	0
$w_{2,3}$	$18.43 \frac{T^2}{E}$	$-28.53 \frac{T^2}{E}$	$-10.24 \frac{T^2}{E}$	0	0	0	0
$w_{2,5}$	$7.314 \frac{T^2}{E}$	$34.13 \frac{T^2}{E}$	$-41.89 \frac{T^2}{E}$	0	0	0	0
$w_{2,7}$	$4.779 \frac{T^2}{E}$	$18.03 \frac{T^2}{E}$	$49.68 \frac{T^2}{E}$	0	0	0	0
$w_{3,2}$	$638.2h^2$	0	0	$14.63 \frac{T^2}{E}$	$-28.33 \frac{T^2}{E}$	$-10.45 \frac{T^2}{E}$	$-6.827 \frac{T^2}{E}$
$w_{3,4}$	0	$1205h^2$	0	$5.851 \frac{T^2}{E}$	$37.63 \frac{T^2}{E}$	$-48.76 \frac{T^2}{E}$	$-18.62 \frac{T^2}{E}$
$w_{3,6}$	0	0	$1985h^2$	$3.762 \frac{T^2}{E}$	$14.63 \frac{T^2}{E}$	$58.84 \frac{T^2}{E}$	$-70.89 \frac{T^2}{E}$
$w_{4,1}$	$14.63 \frac{T^2}{E}$	$5.851 \frac{T^2}{E}$	$3.762 \frac{T^2}{E}$	$2355h^2$	0	0	0
$w_{4,3}$	$-28.33 \frac{T^2}{E}$	$27.62 \frac{T^2}{E}$	$14.63 \frac{T^2}{E}$	0	$2743h^2$	0	0
$w_{4,5}$	$-10.45 \frac{T^2}{E}$	$-48.76 \frac{T^2}{E}$	$58.84 \frac{T^2}{E}$	0	0	$3807h^2$	0
$w_{4,7}$	$-6.827 \frac{T^2}{E}$	$18.63 \frac{T^2}{E}$	$-70.89 \frac{T^2}{E}$	0	0	0	$5136h^2$
$w_{1,2}^2$	$-2.702w_{1,2}$	$-.08820w_{1,2}$	$-.3509w_{1,2}$	$3.764w_{2,1}$	$1.913w_{2,1}$	$-.05447w_{2,1}$	$-.1593w_{2,1}$
$w_{1,2}^2$	$-.2637w_{1,4}$	$-10.04w_{1,2}$	$-.1818w_{1,4}$	$-14.23w_{2,3}$	$-13.25w_{2,3}$	$-.4101w_{2,3}$	$.01283w_{2,3}$
$w_{1,4}^2$	$-.8943w_{1,4}$	$-.40.85w_{1,4}$	$-.1050w_{1,4}$	$-47.36w_{2,1}$	$-1.806w_{2,1}$	$-.1.396w_{2,1}$	$-11.36w_{2,1}$
$w_{1,4}^2$	$-40.80w_{1,2}$	$-.8272w_{1,2}$	$-4.871w_{1,2}$	$-3.572w_{2,3}$	$-41.93w_{2,3}$	$-10.04w_{2,3}$	$-.9079w_{2,3}$
$w_{2,1}^2$	$37.42w_{1,2}$	$-15.12w_{1,2}$	$1.982w_{1,2}$	$-1.384w_{2,1}$	$.1185w_{2,1}$	$-.05108w_{2,1}$	$-.05816w_{2,1}$
$w_{2,1}^2$	$-59.49w_{1,4}$	$97.11w_{1,4}$	$-42.18w_{1,4}$	$7.272w_{2,3}$	$-8.927w_{2,3}$	$.8521w_{2,3}$	$-.01417w_{2,3}$
$w_{2,3}^2$	$59.78w_{1,2}$	$11.14w_{1,2}$	$-.9001w_{1,2}$	$-0.07261w_{2,3}$	$-1.004w_{2,3}$	$-.1597w_{2,3}$	$.001370w_{2,3}$
$w_{2,3}^2$	$113.9w_{1,4}$	$112.9w_{1,4}$	$-1.018w_{1,4}$	$-15.13w_{2,1}$	$-.07163w_{2,1}$	$-1.037w_{2,1}$	$.2923w_{2,1}$
$w_{1,2}w_{1,4}w_{2,1}$	0	0	0	28.11	6.550	7.452	.4739
$w_{1,2}w_{1,4}w_{2,3}$	0	0	0	-38.47	-53.60	-39.94	-.7123
$w_{1,2}w_{2,1}w_{2,3}$	56.17	56.97	-29.88	0	0	0	0
$w_{1,4}w_{2,1}w_{2,3}$	101.5	11.02	90.47	0	0	0	0

Table 2 - Values of deflection coefficients as a function of apparent shearing deformation $\bar{\gamma}$ or of shear load Q

$\frac{Qa^2}{Eh^3b}$	$-\bar{\gamma} \frac{a^2}{h^2}$	$\frac{T_a^2}{Eh^2}$	$\frac{w_{1,2}}{h}$	$\frac{w_{1,4}}{h}$	$\frac{w_{2,1}}{h}$	$\frac{w_{2,3}}{h}$	$\frac{w_{3,2}}{h}$	$\frac{w_{3,6}}{h}$	$\frac{w_{2,5}}{h}$	$\frac{w_{2,7}}{h}$	$\frac{w_{3,4}}{h}$	$\frac{w_{3,6}}{h}$	$\frac{w_{4,1}}{h}$	$\frac{w_{4,3}}{h}$	$\frac{w_{4,5}}{h}$	$\frac{w_{4,7}}{h}$
5.54	0	-5.54	0	0	0	0	0	0	0	0	0	0	0	0	0	0
5.55	14.62	-5.55	0.050	-0.010	0.010	-0.016	-0.003	-0.001	0.000	0.000	0.002	0.000	0.000	0.000	0.000	0.000
5.61	14.78	-5.61	.100	-.020	.020	-.032	-.005	-.002	.000	.000	.003	.001	.000	.001	.000	.000
5.74	15.16	-5.76	.200	-.041	.039	-.065	-.011	-.004	-.001	.000	.007	.002	.001	-.001	.000	.000
6.00	15.90	-6.04	.300	-.064	.057	-.101	-.017	-.007	-.001	.000	.012	.003	.001	-.001	-.001	.000
6.32	16.88	-6.41	.400	-.092	.074	-.143	-.025	-.011	.000	.001	.018	.004	.002	-.002	-.001	-.001
6.50	18.31	-6.95	.500	-.132	.086	-.196	-.035	-.015	.004	.002	.029	.006	.002	-.002	-.001	-.001
7.10	19.21	-7.30	.550	-.158	.090	-.228	-.042	-.018	.008	.004	.037	.007	.002	-.002	-.001	-.001
7.44	20.22	-7.68	.600	-.182	.094	-.260	-.049	-.021	.009	.004	.043	.008	.003	-.002	-.002	-.001
7.82	21.36	-8.12	.650	-.209	.096	-.295	-.058	-.025	.011	.005	.050	.009	.003	-.002	-.002	-.002
8.24	22.68	-8.61	.700	-.239	.098	-.334	-.068	-.029	.013	.006	.059	.011	.004	-.003	-.002	-.002
9.30	25.91	-9.84	.800	-.310	.097	-.424	-.093	-.040	.018	.008	.081	.015	.006	-.004	-.003	-.003
10.60	29.98	-11.39	.900	-.395	.092	-.531	-.126	-.054	.024	.011	.110	.021	.007	-.005	-.004	-.003
12.22	35.08	-13.33	1.000	-.489	.083	-.652	-.171	-.073	.032	.015	.149	.028	.009	-.007	-.006	-.005
14.12	41.11	-15.62	1.100	-.585	.076	-.780	-.227	-.096	.043	.020	.197	.037	.012	-.009	-.008	-.006
16.36	48.32	-18.36	1.200	-.697	.067	-.920	-.295	-.125	.056	.026	.257	.048	.016	-.012	-.010	-.008
18.60	55.54	-21.10	1.300	-.775	.065	-1.054	-.376	-.160	.071	.033	.327	.061	.020	-.015	-.013	-.010
21.18	63.93	-24.29	1.400	-.867	.062	-1.199	-.471	-.200	.089	.041	.410	.077	.025	-.018	-.016	-.013
23.97	73.12	-27.76	1.500	-.959	.060	-1.351	-.585	-.248	.111	.051	.510	.096	.031	-.023	-.020	-.016

Table 3 - Median Fiber Stresses at Center, Maximum and Minimum Principal Stresses, and Direction of Maximum Principal Stress

$\frac{qa^2}{Eh^3b}$	$\frac{\sigma'_x a^2}{Eh^2}$	$\frac{\sigma'_y a^2}{Eh^2}$	$\frac{\tau'_{xy} a^2}{Eh^2}$	$\frac{\sigma'_{min} a^2}{Eh^2}$	$\frac{\sigma'_{max} a^2}{Eh^2}$	α^*
5.55	.01	.00	-5.55	-5.53	5.59	44°59'
5.61	.03	.02	-5.59	-5.57	5.61	44°58'
5.74	.12	.06	-5.68	-5.58	5.75	44°52'
6.00	.27	.15	-5.84	-5.61	6.03	44°42'
6.32	.50	.27	-6.04	-5.62	6.39	44°26'
6.80	.86	.45	-6.33	-5.62	6.93	44° 6'
7.10	1.09	.58	-6.50	-5.61	7.28	43°51'
7.44	1.35	.71	-6.70	-5.61	7.67	43°37'
7.82	1.66	.86	-6.92	-5.59	8.12	43°20'
8.24	2.02	1.04	-7.16	-5.56	8.63	43° 2'
9.30	2.94	1.49	-7.76	-5.48	9.92	42°20'
10.60	4.20	2.08	-8.46	-5.27	11.56	41°25'
12.22	5.85	2.82	-9.29	-4.98	13.65	40°22'
14.12	7.93	3.67	-10.26	-4.57	16.17	39° 8'
16.36	10.53	4.75	-11.30	-3.90	19.18	37°50'
19.60	13.48	5.64	-12.32	-3.26	22.38	36°11'
21.18	17.06	6.73	-13.41	-2.37	26.17	34°28'
23.97	21.31	7.88	-14.51	-1.28	30.48	32°34'

* α angle between direction of maximum principal stress and flanges.

Table 4 - Stresses at upper corner of Shear Web, towards Which Wrinkles Point,
 $x=0$, $y=b$ and effective width ratio

$\frac{Qa^2}{Eh^3b}$	$\frac{\sigma_x'a^2}{Eh^2}$	$\frac{\sigma_y'a^2}{Eh^2}$	$\frac{\tau_{xy}'a^2}{Eh^2}$	$\frac{\sigma_{\min}'a^2}{Eh^2}$	$\frac{\sigma_{\max}'a^2}{Eh^2}$	$\frac{\tau_{xy}''a^2}{Eh^2}$	α^*	Effective width ratio
5.55	0.00	0.00	5.55	-5.55	5.54	-0.22	44°59'	1.000
5.61	.00	-.01	5.61	-5.62	5.61	-.44	44°59'	.999
5.74	-.01	-.03	5.76	-5.78	5.74	-.90	44°57'	.996
6.00	-.02	-.07	6.04	-6.09	6.00	-1.38	44°54'	.992
6.32	-.05	-.12	6.41	-6.50	6.33	-1.89	44°49'	.986
6.80	-.08	-.21	6.96	-7.10	6.81	-2.43	44°44'	.978
7.10	-.10	-.26	7.30	-7.48	7.12	-2.70	44°41'	.973
7.44	-.13	-.32	7.68	-7.91	7.46	-3.02	44°38'	.968
7.82	-.16	-.40	8.12	-8.39	7.84	-3.36	44°34'	.963
8.24	-.19	-.49	8.62	-8.96	8.27	-3.73	44°30'	.957
9.30	-.29	-.73	9.84	-10.36	9.34	-4.54	44°21'	.944
10.60	-.42	-.107	11.39	-12.14	10.65	-5.49	44°11'	.931
12.22	-.60	-.154	13.33	-14.41	12.26	-6.49	43°59'	.917
14.12	-.83	-.214	15.62	-17.12	14.15	-7.76	43°48'	.904
16.36	-.1.12	-.2.91	18.36	-20.40	16.37	-9.03	43°36'	.892
18.60	-.1.41	-.3.72	21.10	-23.70	18.56	-10.48	43°26'	.882
21.18	-.1.78	-.4.72	24.29	-27.58	21.09	-12.04	43°16'	.872
23.97	-.2.19	-.5.87	27.78	-31.87	23.81	-13.75	43°6'	.863

* angle between direction of maximum principal stress and flanges.

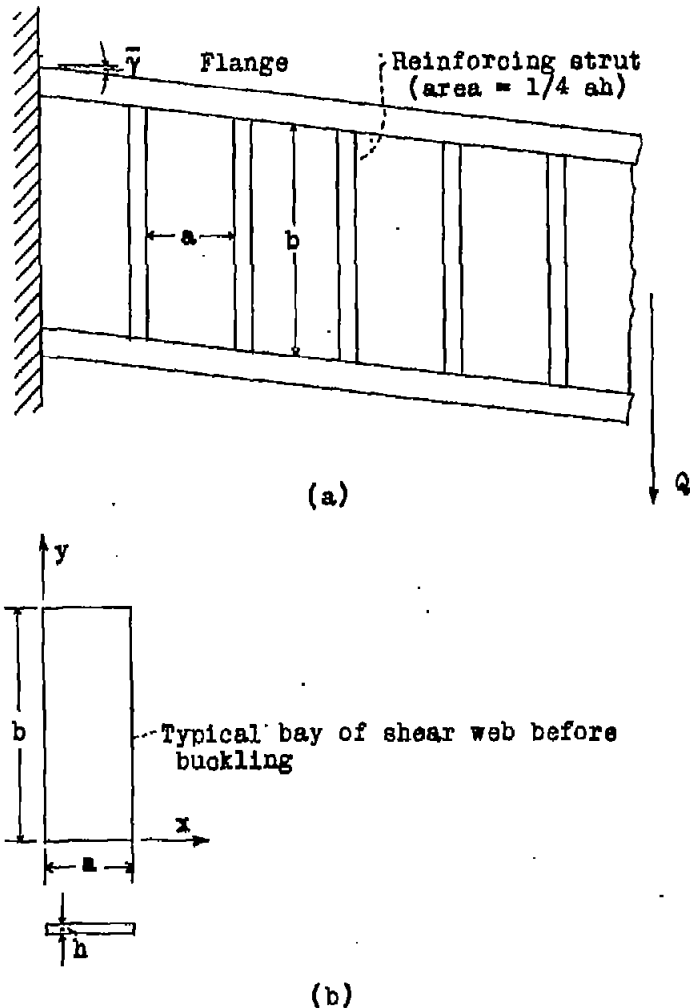


Figure 1.- Beam under shearing force Q and typical bay of shear web.

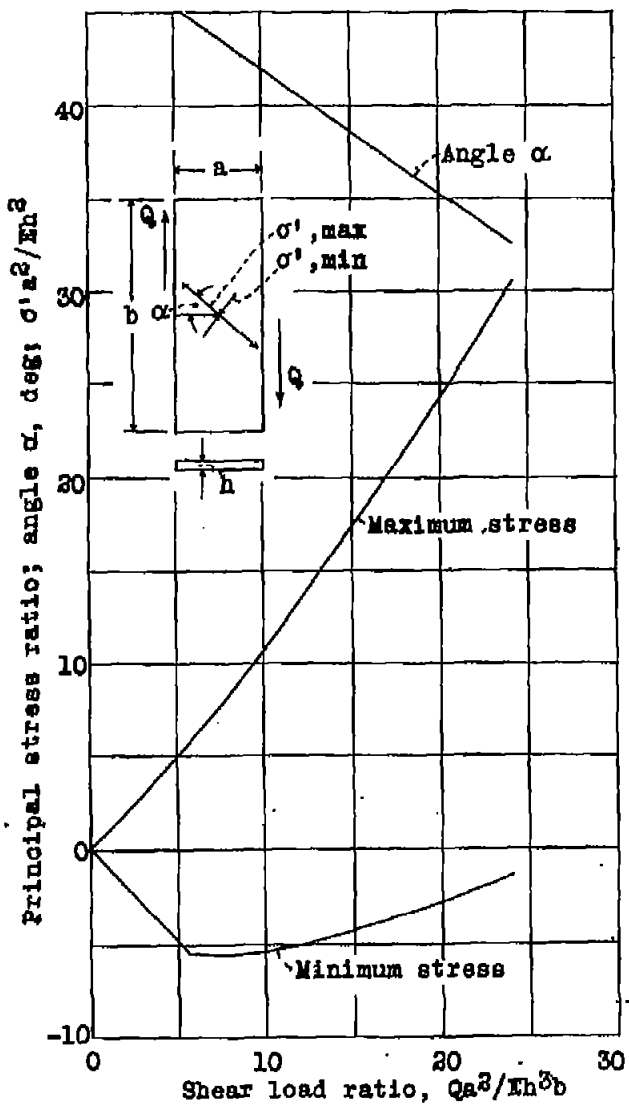


Figure 2.- Principal median fiber stresses at center of shear bay and direction of maximum principal stress. Bending stresses are zero at center of bay.

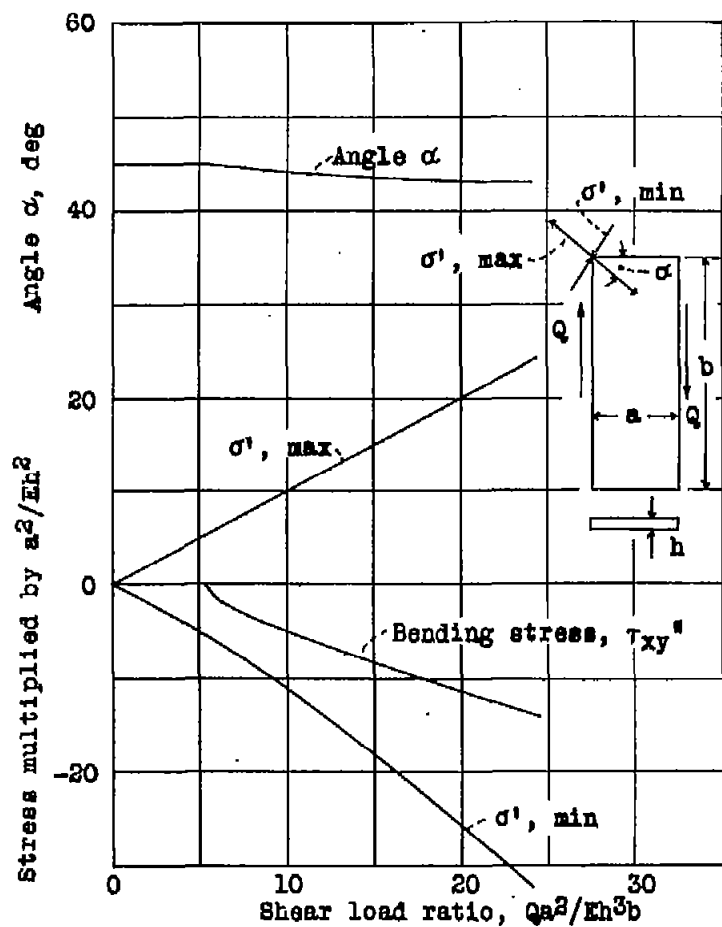


Figure 3.- Principal median fiber stresses and bending stresses at corner of shear bay, and direction of maximum principal median fiber stress. Bending stresses σ_x^1 and σ_y^1 are zero at corner.

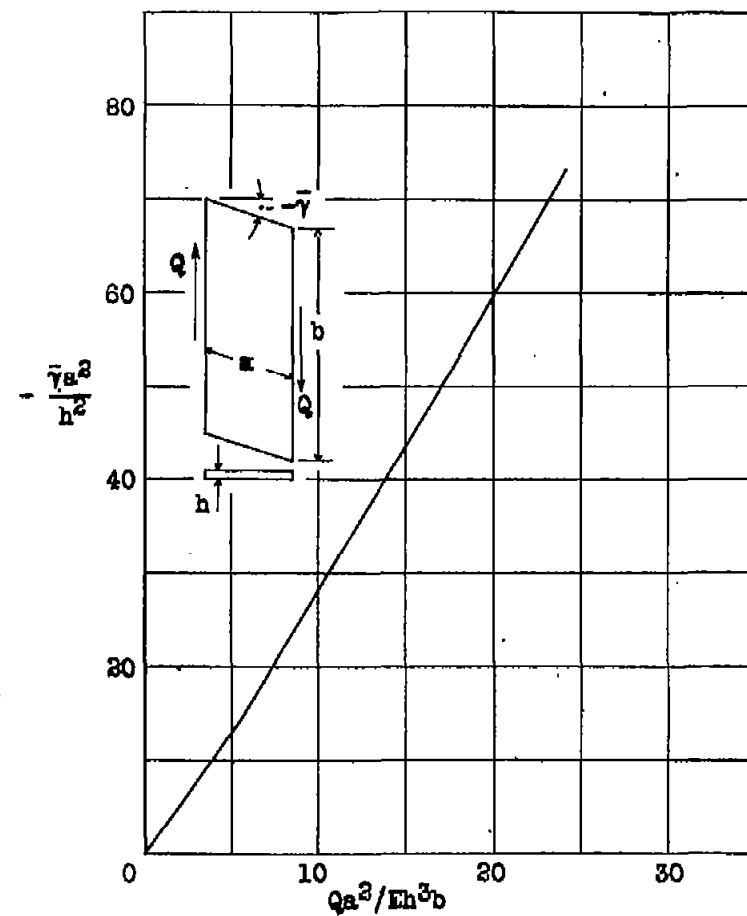


Figure 4.- Shear deformation of beam as a function of load.

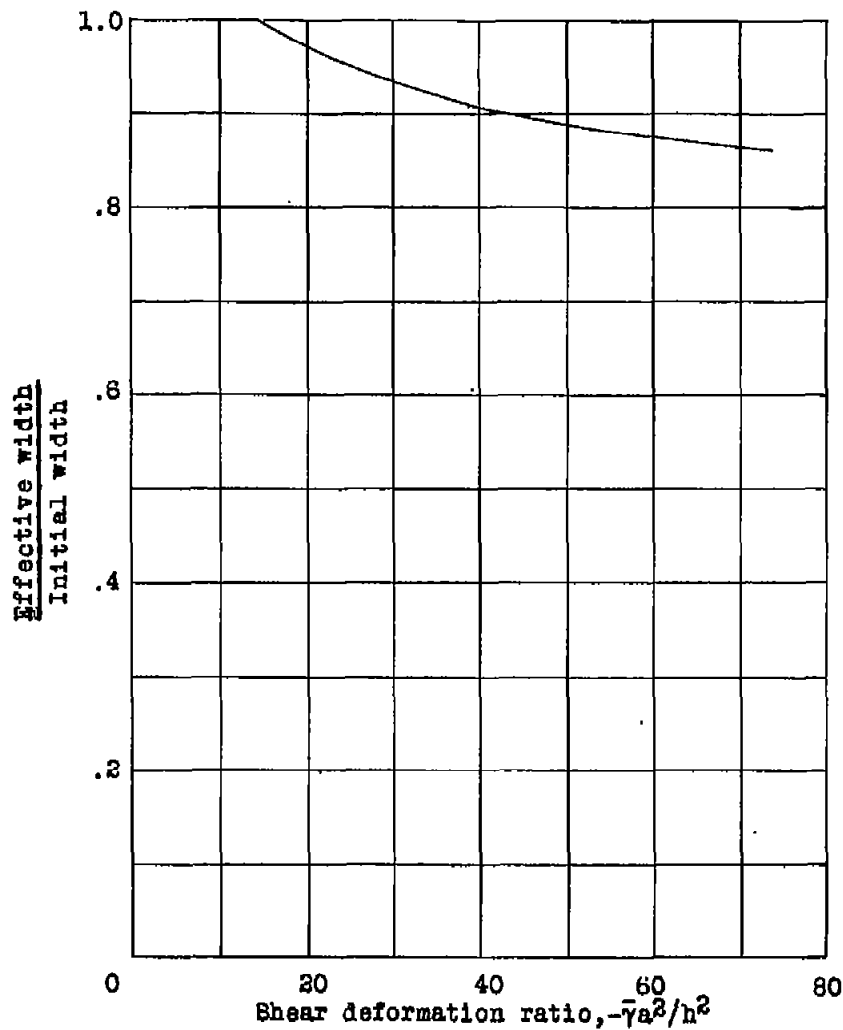


Figure 5. - Effective width of sheet after buckling.

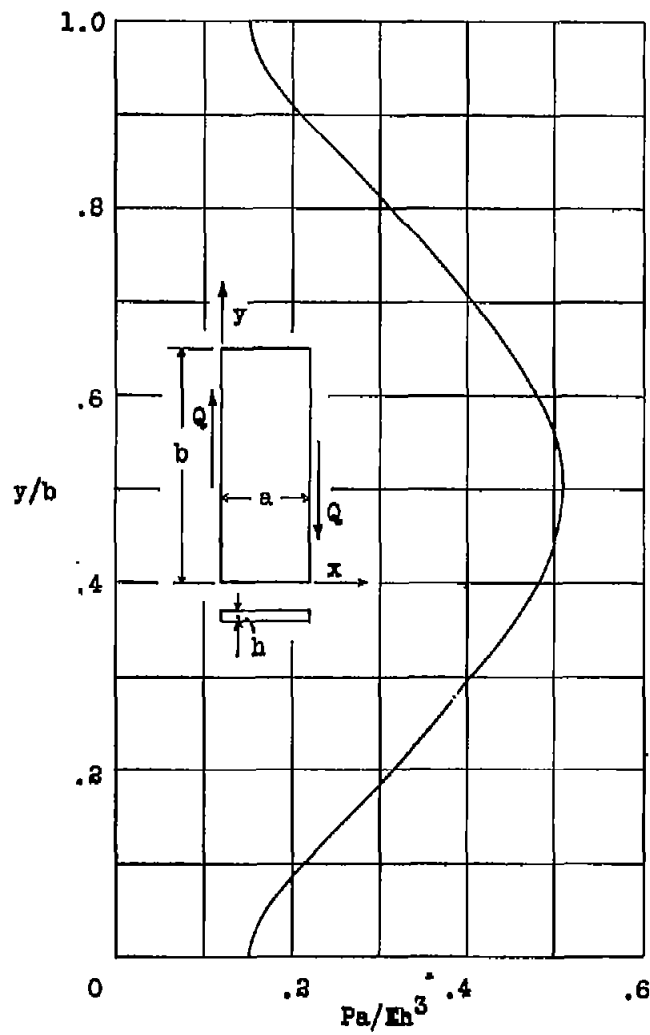


Figure 6. - Distribution of force P in struts at $x = 0, a$ when $Q = 9 \cdot 30 Eh^3 b/a^2$.

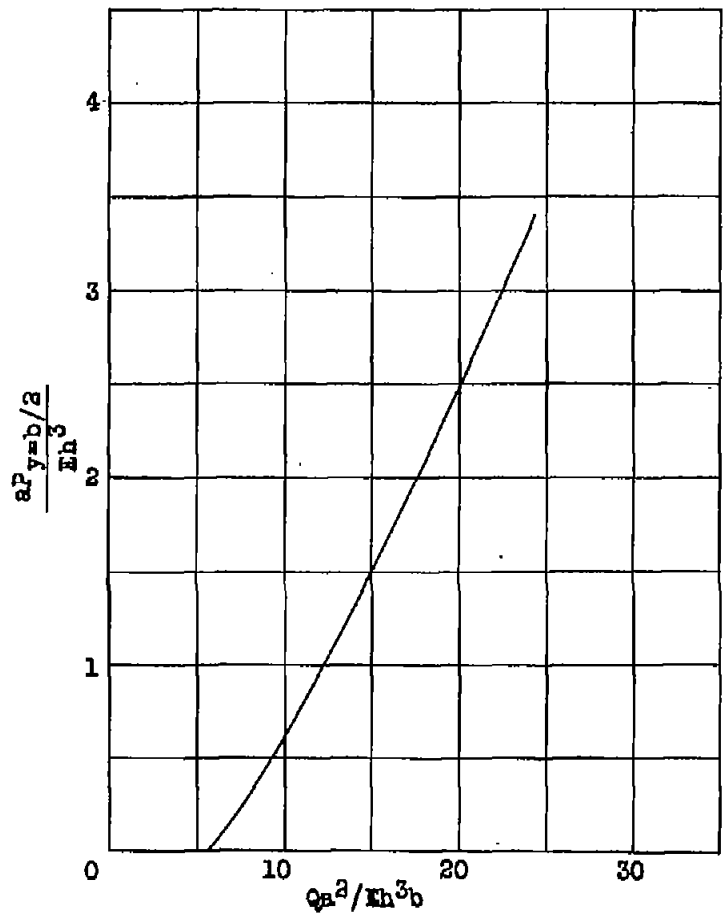


Figure 7.- Variation of compressive force $P_{y=b/2}$ at midpoint of strut with shear load Q .

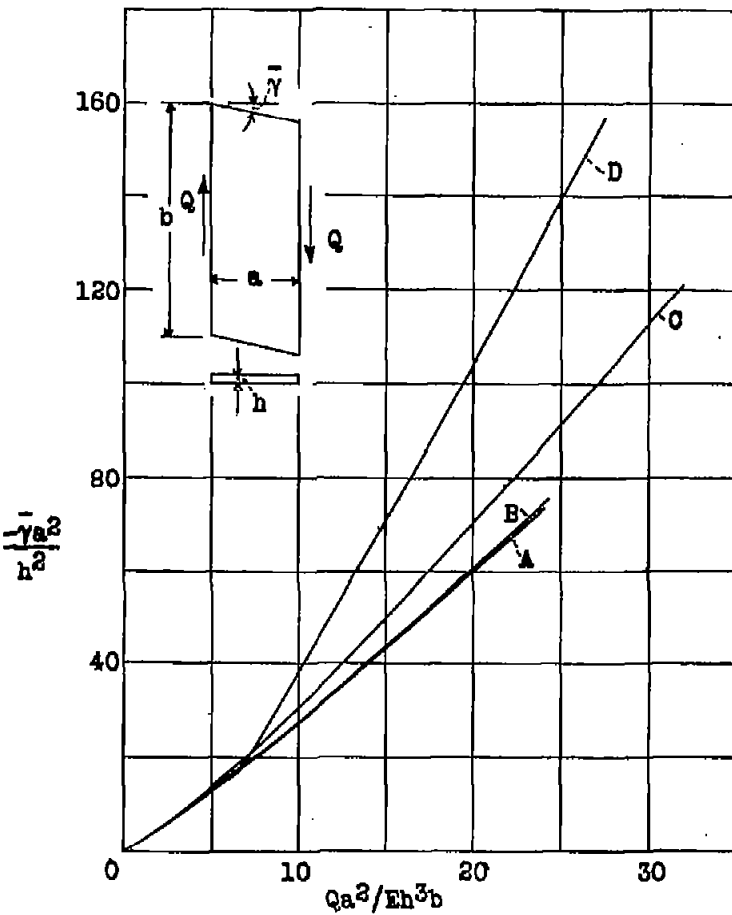


Figure 8.- Shear deformation, $-\bar{\gamma}$ versus shearing force Q for shear webs with reinforcement ratio $r = 1/4$. Curve A: present analysis, $b/a = 2.5$; curve B: reference 1, $b/a = 1$; curve C: reference 6, $b/a = 2.5$; curve D: reference 7, $b/a = 2.5$.

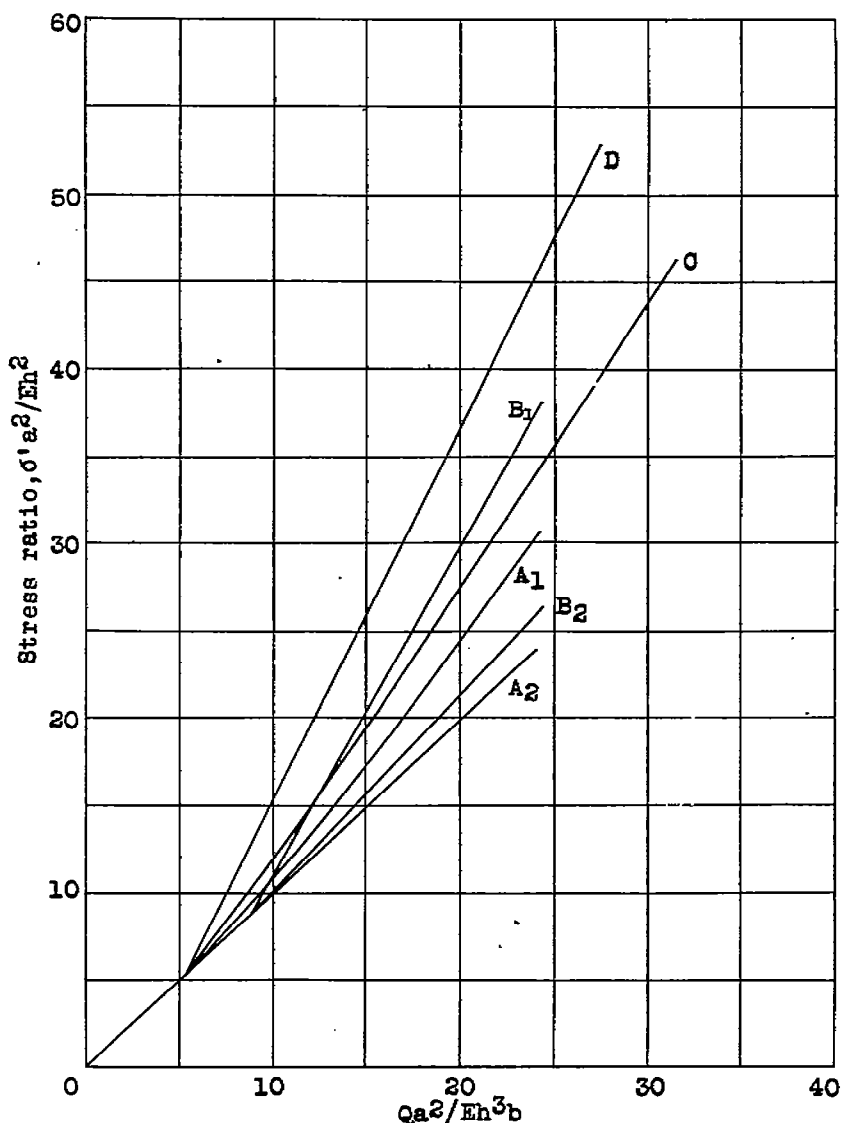


Figure 9.- Maximum median fiber stress versus shearing force for shear webs with reinforcement ratio, $r = 1/4$. Curve A₁: present analysis, center of plate, $b/a = 2.5$; curve A₂: present analysis, corner of plate in line with diagonal tension wrinkles, $b/a = 2.5$; curve B₁: reference 1, center of plate, $b/a = 1$; curve B₂: reference 1, corner of plate in line with diagonal tension wrinkles, $b/a = 1$; curve C: reference 6, throughout plate, $b/a = 2.5$; curve D: reference 7, throughout plate, $b/a = 2.5$.

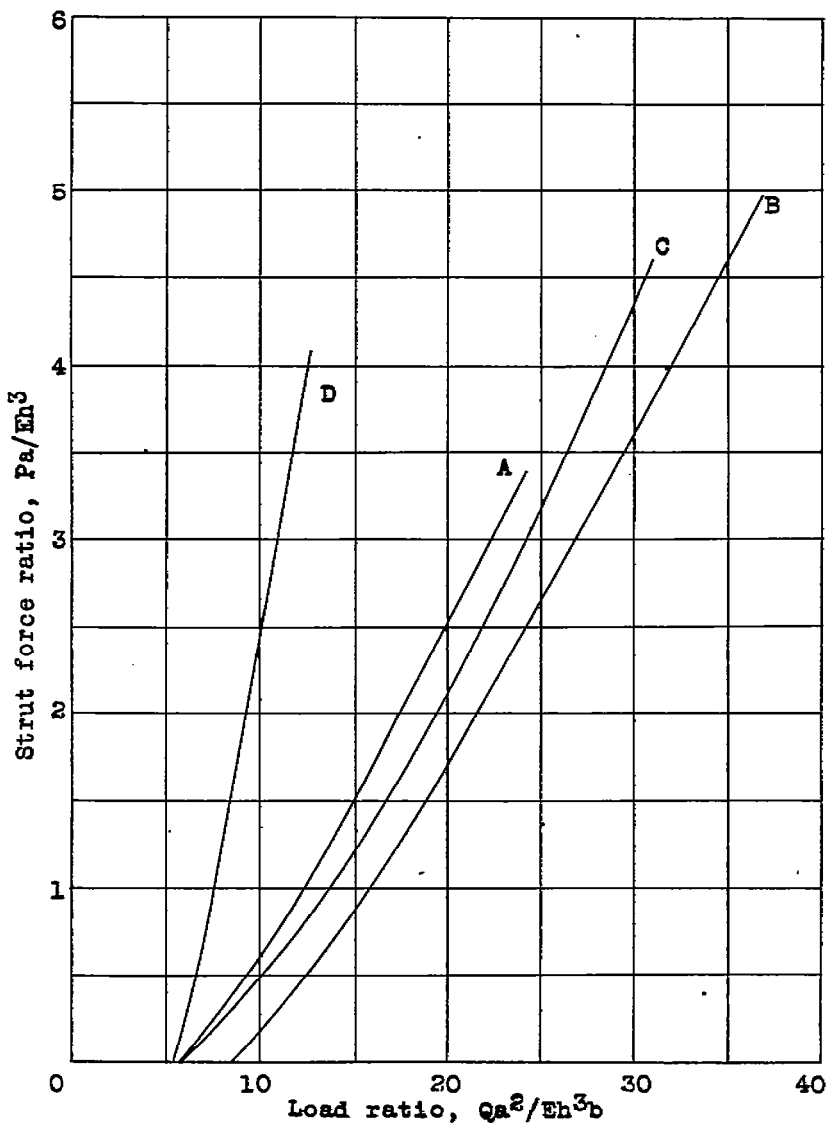


Figure 10.- Strut force P versus shearing force Q for shear webs with reinforcement ratio, $r = 1/4$. Curve A: present analysis, mid-point of strut, $b/a = 2.5$; curve B: reference 1 analysis, mid-point of strut, $b/a = 1$; curve C: reference 6 analysis, throughout strut, $b/a = 2.5$; curve D: reference 7 analysis, throughout strut, $b/a = 2.5$.